ORIGINAL RESEARCH

Identification of Novel Targets for Treatment of Dilated Cardiomyopathy Based on the Ferroptosis and Immune Heterogeneity

Hongyu Lu[1,2,*], Yun Xie[1,3,*], Ziyou Zhou [1,4,*], Peijian Hong [5,*], Jiyan Chen[1,2]

[1]Department of Cardiology, Guangdong Cardiovascular Institute, Guangdong Provincial People's Hospital, Guangdong Academy of Medical Sciences, Guangzhou, People's Republic of China; [2]Department of Guangdong Provincial Key Laboratory of Coronary Heart Disease Prevention, Guangdong Cardiovascular Institute, Guangdong Provincial People's Hospital, Guangdong Academy of Medical Sciences, Southern Medical University, Guangzhou, People's Republic of China; [3]School of Biology and Biological Engineering, South China University of Technology, Guangzhou, People's Republic of China; [4]School of medicine, South China University of Technology, Guangzhou, People's Republic of China; [5]Department of Histology and Embryology School of Basic Medicine, Tongji Medical College, Huazhong University of Science and Technology, Wuhan, People's Republic of China

*These authors contributed equally to this work

Correspondence: Jiyan Chen, Department of Cardiology, Guangdong Provincial Key Laboratory of Coronary Heart Disease Prevention, Guangdong Cardiovascular Institute, Guangdong Provincial People's Hospital, Guangdong Academy of Medical Sciences, Guangzhou, People's Republic of China, Tel + (86)02083827812-10528, Fax + (86)02083851483, Email chen-jiyan@163.com

Purpose: This study aimed to investigate the role of ferroptosis in dilated cardiomyopathy (DCM) and to identify new targets for treatment and diagnosis of DCM.

Methods: GSE116250 and GSE145154 were downloaded from the Gene Expression Omnibus database. Unsupervised consensus clustering of DCM patients was used to confirm the impact of ferroptosis. Ferroptosis-related hub genes were identified by WGCNA and single cell sequencing analyses. Finally, we established a DCM mouse model via injection of Doxorubicin to verify the expression level of *OTUD1* and colocalization between cell markers and *OTUD1* in DCM mouse heart.

Results: A total of 13 ferroptosis-related differentially expressed genes (DEGs) were identified. The DCM patients were divided into two clusters according to the expression of 13 DEGs. The DCM patients in different clusters showed discrepancies in immune infiltration. Four hub genes were further identified by WGCNA analysis. Single cell data analysis revealed that *OTUD1* may regulate B cells and DC cells and then participate in immune infiltration discrepancy. The upregulation of *OTUD1* and the colocalization of *OTUD1* with CD19 (B cell maker) and CD11c (DCs markers) markers were confirmed in DCM mouse hearts.

Conclusion: Ferroptosis and the immune microenvironment are closely associated with DCM, and *OTUD1* may play an important role through B cells and DCs.

Keywords: dilated cardiomyopathy, ferroptosis, immune infiltrations, single cell sequencing

Introduction

Dilated cardiomyopathy (DCM) is one of the leading causes of heart failure (HF). Patients with DCM usually appear to have left ventricular dilatation and systolic dysfunction, but in the absence of diagnosis of abnormal load conditions and severe coronary artery disease.[1] At present, the etiology of DCM has not been clarified, studies have shown that genetic aspects, infectious agents, metabolism, drugs and toxins are important causes of DCM and that these factors can interact with each other leading to the occurrence of DCM.[1] So far, there is no effective treatment to prevent the progression of DCM due to the complexity of the causes. Studies have revealed that many pathogenic pathways, including metabolism and immunological inflammation, are connected to the incidence and progression of DCM.[2–4] A variety of cell deaths have been reported to be involved in the development of DCM including apoptosis, autophagy and pyroptosis.[5–7] However, as one of the important types of cell death, the role of ferroptosis in DCM has not been clearly elucidated. Ferroptosis is a type of cell death depending on reactive oxygen species (ROS) and mainly characterized by iron accumulation and lipid peroxidation.[8] Ferroptosis occurs through two main

pathways, including extrinsic or transporter-dependent pathways such as reduced glutamine uptake, and intrinsic or enzyme-regulated pathways such as inhibition of GPX4, both of which can lead to a decrease in antioxidant capacity and increased susceptibility of cells to ferroptosis.[9] Evidence has shown that ferroptosis plays an important role in various cardiovascular diseases such as chronic heart failure and myocardial ischemia-reperfusion injury.[10,11] For example, Miyamoto et al demonstrated iron overload via heme degradation in the endoplasmic reticulum will trigger ferroptosis in myocardial ischemia-reperfusion injury.[12] However, few studies have focused on the relationship between ferroptosis and DCM.[13]

DCM is highly associated with the immune system. Existing evidence suggests that patients with DCM have heterogeneity, including immune heterogeneity, which results in different sensitivity to treatment.[14] Immune infiltration is defined as the aggregation and accumulation of immune cells such as T cells, B cells and DC cells within the tissues.[15] According to the previous research, immune heterogeneity is highly related to immune infiltration because the type and abundance of immune cells within tissues can contribute to the overall immune heterogeneity of the region.[16] Meanwhile, previous studies have found that ferroptosis is strongly associated with heterogeneity in patients with lung adenocarcinoma, especially in immune heterogeneity.[17] Therefore, ferroptosis may also play a role in the occurrence of immune heterogeneity in DCM patients and ferroptosis-related genes may be new targets for the treatment of DCM.

In this study, we conducted unsupervised consensus clustering of DCM patients based on ferroptosis-related gene expression, and further identified hub genes by WGCNA analysis. In order to clarify the putative immunological mechanism of ferroptosis in DCM, we simultaneously examined the immune infiltration variety across patients in different clusters and concentrated on the potential function of hub genes in the immune microenvironment. Finally, we constructed a DCM mouse model and verified the expression level and cellular colocation of hub genes.

Materials and Methods
Animal Model
C57BL/6J mice (10 weeks, male) were obtained from South China University of Technology (Guangzhou, China). Mice were given injections of doxorubicin (Dox) or saline at a total dosage of 12 mg/kg (4 mg/kg i.P. at 0, 7, and 14 days) for three weeks. Six weeks following the initial injection, cardiac function was evaluated. All mice were kept in certified specific pathogen-free facilities and received free food and water. At the end of the experiment, the heart samples of the mice were collected. The animal experiments were approved by the Animal Care and Use Committee of Guangdong Provincial People's Hospital. The experiment complied with the Guide for the Care and Use of Laboratory Animals published by the US National Institutes of Health (NIH Publication No. 85–23, revised 1996).

Mouse Echocardiography
The mice were anesthetized with 3% isoflurane and echocardiography was performed to access the systolic function using the Visualsonics imaging system (Vivo 2100, Toronto, Canada).

RNA Isolation and Real-Time Quantitative PCR (RT-qPCR)
Total RNAs were isolated from mouse hearts section sample using a TRIzol reagent (TAKARA, Japan). cDNA was synthesized via reverse transcription using a PrimeScript™ RT Reagent Kit (TAKARA, Japan) with random 6mers and oligo dT primers according to the manufacturer's protocol (Takara, Japan). The relative expression of the target genes was normalized to GAPDH mRNA. All reactions were repeated in triplicate and the result was shown as means ± SD. The primer sequences were shown as follows:
*OTUD1*_forward: CGACGTGGGGGGAGTTTATTA;
*OTUD1*_reverse: GCCCAGATAGTGGATCATGG;
GAPDH_forward: AGGTCGGTGTGAACGGATTTG;
GAPDH_reverse: TGTAGACCATGTAGTTGAGGTCA.

GSH/GSSG Assay

The ratio of GSH/GSSG was measured according to the instruction of the assay kit (byotime, S0053), then detected at 412 nm via Varioskan Lux (ThermoFisher, USA).

Western Blot Analysis

The samples were lysed in RIPA buffer, and protein levels were quantified using a BCA protein assay kit (Beyotime, China). The protein was separated by SDS-PAGE, electrotransferred to PVDF membranes, incubated with primary antibodies at 4°C overnight, washed three times, incubated for 1 hour with secondary antibodies at room temperature, and visualized by chemiluminescence reagents. Anti-OTUD1 (bs-17563R) antibody was purchased from Bioss (China) and anti-GPX4 (67763-1-Ig) antibody was purchased from proteintech (USA).

Immunofluorescence Staining

Heart sections were blocked with 3% H2O2 for 15 min and then with goat serum (10%) for 1 h after antigen retrieval. Subsequently, the sections were incubated with the primary antibodies at 4°C overnight followed by secondary antibodies. Nuclei were stained using DAPI (Beyotime, China). Angiogenesis was observed using a confocal microscope (Olympus, Japan).

The primary antibodies used are as follows: OTUD1 (bs-17563R, 1:200, Bioss, China), CD19 (14–0194-82, 1:100, ThermoFisher, USA), 4-hydroxynonenal (4-HNE) (ab3517, Abcam, Cambridge, UK).

The secondary antibodies used are as follows: Goat Anti-Mouse IgG H&L (TRITC) (115–025-062, 1:200, Jackson ImmunoResearch, USA), Goat Anti-Rabbit IgG H&L (FITC) (111–095-003, 1:200, Jackson ImmunoResearch, USA), Goat Anti-Rat IgG H&L (TRITC) (112–585-003, 1:200, Jackson ImmunoResearch, USA).

Data Source

Gene expression data sets were searched using dilated cardiomyopathy as the key phrase. The subsequent standards were applied during screening: 1. Patients with clinically confirmed DCM. 2. Data sets should include patients and healthy controls and should include as many samples as possible. 3. Human heart tissue should be used for the test specimens in the dataset. The Series Matrix File Data File of GSE116250 was downloaded from NCBI GEO public database, and the annotation platform was GPL16791. A total of 51 transcriptome data were collected, comprising 14 control samples and 37 DCM samples. Single cell data of GSE145154 were downloaded from NCBI GEO public database, and a total of 12 samples (including 4 control samples and 8 DCM samples) were used for analysis. Ferroptosis-related genes were collected from GeneCards database.

Differential Expression Analysis

Differential expression analysis was performed using the latest version of the "Limma" package in R 4.0.3 software. Fold change (FC) was calculated according to the average gene expression in DCM group and control group. The differentially expressed genes were defined by the cutoff values ($|logFC|>1$ and $P < 0.05$).

Functional Enrichment Analysis of Differential Genes

To comprehensively explore the functional correlation of these differentially expressed genes (DEGs), R package "clusterProfiler" was used to annotate the differentially expressed genes. Gene Ontology (GO) and Kyoto Encyclopedia of Genes and Genomes (KEGG) were used to assess pertinent functional categories. The GO and KEGG pathways with p value <0.05 and q value <0.05 were considered to be significant categories. The background gene set consists of c5.go.v7.5.1.entrez.gmt and c2.cp.kegg.v7.5.1.entrez.gmt.

Consensus Clustering Analysis

Based on the expression levels of differential expressed ferroptosis genes, DCM samples were clustered by the consistent clustering method. Each iteration of the clustering process, which involved 10 iterations, contained 80% of the data. The

optimal number of clusters was calculated by the cumulative distribution function curve of the consistency score and the characteristics of the consistency matrix heat map.

Immune Infiltration Analysis

To evaluate the effect of differentially expressed ferroptosis genes on immune infiltration, ssGSEA was used to assess the degree of immune cell infiltration in each sample. Pearson correlation analysis was performed on gene expression and immune cell content. $P < 0.05$ was considered statistically significant.

WGCNA Network Construction

The co-expression network of all genes in the GSE116250 dataset was constructed using the WGCNA-R package. The first 5000 highly variable genes were screened for further analysis, and the soft threshold was set to 8. The weighted adjacency matrix was converted into topological overlap matrix (TOM) to estimate the network connectivity, and the hierarchical clustering was used to construct the clustering tree structure of TOM matrix. Based on the weighted correlation coefficients, genes were classified according to the respective expression patterns, and genes with similar patterns were grouped into a module.

Single-Cell Sequencing Analysis

Seurat package was utilized for quality control and subsequent analysis of the data. The location relationship between each cluster was obtained by UMAP algorithm analysis and the clusters were annotated by MonacoImmuneData file. Finally, we used the FindAllMarkers function to screen the marker genes of each subgroup, among which with | avg_log2FC| > 1 and adjusted p value < 0.05 were considered as unique marker genes in each cell subtype.

Statistical Analysis

A two-sided p-value < 0.05 was considered significant. All analyses were conducted in R software (version 4.1.1) and Prism (version 8.1) for windows 64.0.

Results

Identification and Functional Analysis of Ferroptosis-Related DEGs

The transcriptome data of GSE116250 were retrieved from NCBI GEO public database, and the DEGs between DCM patients and healthy controls were then calculated using the Limma software. After setting the cutoff values, A total of 537 differential genes were screened out, including 292 up-regulated genes and 245 down-regulated genes (Figure 1A and B). A total of 442 ferroptosis-related genes were obtained from Gene cards and 13 genes were screened by intersecting with 537 DEGs (Figure 1C). The 13 ferroptosis-related DEGs were *NQO1, GNB3, MGST1, TUBB4A, G0S2, OTUD1, TGFB2, UCHL1, TPM1, BEX1, HP, TXNRD1* and *XRCC6*. We performed an enrichment analysis of DEGs in order to explore the potential roles of these genes. The results of GO analysis showed that the genes were mostly enriched in the following pathways: extracellular matrix structural constituent, RNA binding involved in posttranscriptional gene silencing, external encapsulating structure organization, collagen fibril organization (Figure 1D). In addition, the KEGG pathway analysis of these DEGs showed that the main pathways with most of the enriched genes were the cardiac muscle contraction, graft versus host disease, type I diabetes mellitus and autoimmune thyroid disease (Figure 1E).

Consensus Clustering Analysis for DCM in Accordance with the Expression of Differential Ferroptosis-Related Genes

In order to advance our understanding about the role of ferroptosis in DCM, we conducted consensus clustering for DCM in view of the 13 differential ferroptosis-related genes. The results showed that the classification among samples was obvious when k = 2. Thus, we eventually separated the DCM sample into two subtypes (Figure 2A), and the CDF value and delta area of all subtypes were also shown (Figure 2B and C).
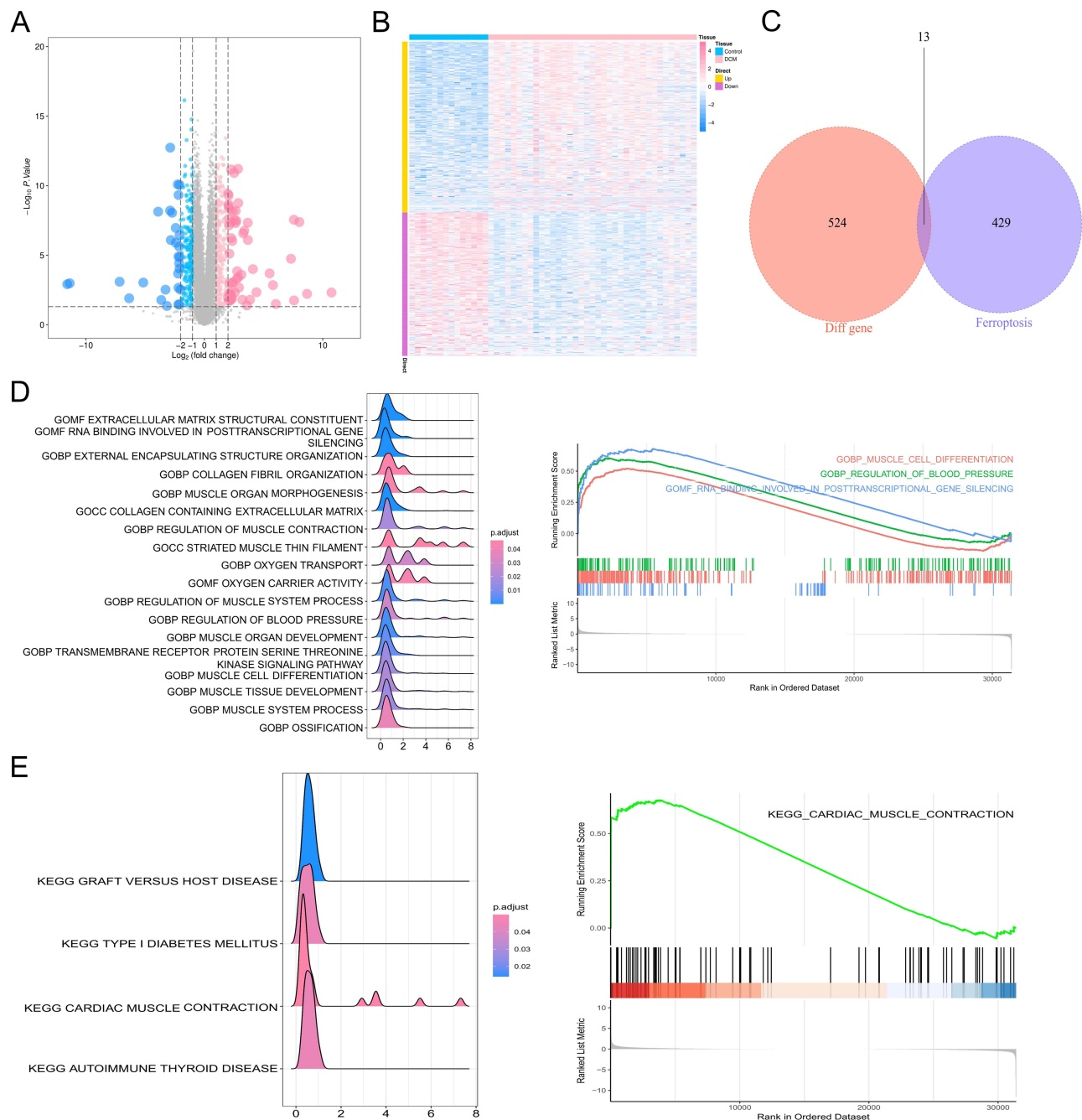
Figure 1 Identification and functional analysis of ferroptosis-related DEGs. (**A**) Volcano plot of 537 DEGs; (**B**) heat map of the DEGs in GSE116250; (**C**) a Venn diagram of GSE116250 DEGs and ferroptosis-related genes; (**D**) the GO enrichment pathway analysis of DEGs; (**E**) the significant KEGG pathways enriched by DEGs.

Identifying and Functional Analysis of Differentially Expressed Genes Between Different Clusters in DCM

To investigate patients' heterogeneity between different ferroptosis subtypes, we performed a GSEA analysis and collected the most representative pathways in cluster1 and cluster2. The heatmap revealed different pathways enriched in each subtype (Figure 2D and E). The highly expressed genes in cluster1 were predominantly enriched in immune-related pathways and metabolism pathways such as immunoglobulin complex circulating, B cell receptor signaling pathway, immunoglobulin complex, antigen binding, tryptophan metabolism and proteasome. In cluster2, the highly
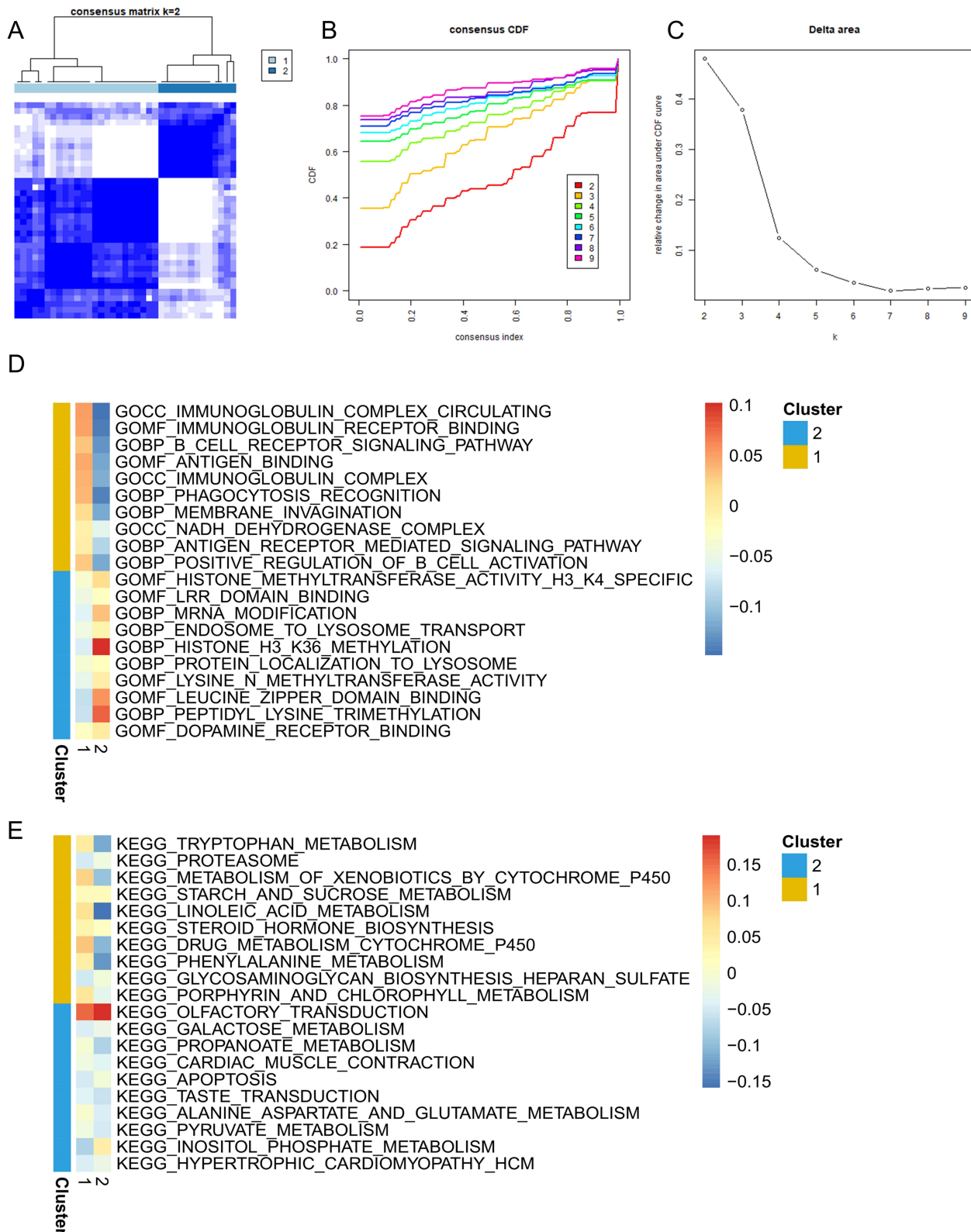
Figure 2 Consensus clustering analysis of DCM and gene set enrichment analysis (GSEA) of the DEGs between two clusters. (**A**) Consistency matrix of samples with k = 2; (**B**) cumulative distribution function of clustering (k, 2–9); (**C**) delta area score displays relative growth in cluster stability; (**D**) GSEA enrichment analysis of GO terms in each cluster; (**E**) GSEA enrichment analysis of KEGG terms in each cluster.

expressed genes were primarily enriched in LRR domain binding, cardiac muscle contraction, pyruvate metabolism, hypertrophic cardiomyopathy. These findings indicated that the cluster defined by ferroptosis-related DEGs had a strong association with heterogeneity, especially immune heterogeneity, in DCM patients.

Immune Infiltration Analysis of the Two Clusters in DCM

To further demonstrate the potential impact of ferroptosis-related genes on the immunological environment of DCM patients, we compared the immune infiltration between the two clusters. The composition of immune cells is depicted in Figure 3A and B cells, DC cells and T helper cells showed significant expression differences between the two clusters, and T helper cells showed a significant increase in expression in cluster1 (Figure 3B). Besides, the correlation of each immune cell significantly increased in cluster1, which further indicated that ferroptosis may affect the immune micro-environment of DCM patients and therefore participated in the immune heterogeneity (Figure 3C and D).

Identification of the Ferroptosis-Related Hub Genes

Next, we further identified the key genes affecting the immune heterogeneity of DCM patients. We constructed WGCNA network based on the expression profile data of GSE116250 to explore the co-expression regulatory network related to DCM. A total of 10 gene modules were detected based on the tom matrix by setting the soft threshold as 8 (Figure 4A and B). The results showed that the red module was most correlated with DCM (Figure 4C). The intersection of 280 genes in the red module and 13 ferroptosis-related DEGs resulted in four hub genes, which were *BEX1, GNB3, OTUD1*, and *TGFB2* (Figure 4D). The expression of the ferroptosis-related hub genes between 2 clusters is shown in Figure 4E.

Single Cell Sequencing Analysis and Orientation of Hub Genes

In order to investigate the role of ferroptosis-related hub genes in immune infiltration, we annotated the data GSE145154 by Single R with MonacoImmuneData as annotation data. All cells were annotated to six types of cells including T cells, Monocytes, NK cells, Progenitors, Dendritic cells (DCs), and B cells (Figure 5A). Expressions of four ferroptosis-related hub genes *BEX1, OTUD1, TGFB2*, and *GNB3*, in each type of cells are shown in Figure 5B. In particular, we found that *OTUD1* was widely expressed in the heart, especially in B cells, DCs, and monocytes. Interestingly, compared with the control group (Figure 5C), the expression proportion and expression level of *OTUD1* in B cells were significantly increased, while those in DCs were significantly decreased (Figure 5D). Detailed descriptions of the remaining 9 DEGs were shown in Supplementary Figure 1. All these data were consistent with previous immune infiltration analysis between different subtypes, which suggested that *OTUD1* may play a vital role in the immune microenvironment of DCM patients and participate in the formation of immune heterogeneity.

Immune Characteristic Analysis of OTUD1

Since we identified *OTUD1* as a key hub gene of DCM, we analyzed the relationship between *OTUD1* and immune regulatory factors, including chemokines, chemokine receptors, immunosuppressants, and immune stimulators in GSE116250 (Figure 6A–D). The results showed *OTUD1* was most relative to TNFSF13B, CCR9, CXCL16, CCL2, and CD274. TNFSF13B has been identified as B cell activator, while CCR9, MICB, and CXCL16 are defined as T cell regulators. Besides, CD274 is expressed in multiple kinds of immune cells including B cells and DCs, and the role of CCL2 in DCs has been widely recognized. In a word, our data suggested *OTUD1* may play an important role in the immune response of DCM.

The Verification of OTUD1 in the Heart of DCM Mice

To confirm the role of *OTUD1* in DCM, a mouse model of DCM was successfully established via Dox injection in accordance with the previous study.[7] The results of echocardiography showed that DOX injection resulted in decreased ejection fraction (EF), shortening fraction (FS), left ventricular posterior wall systolic thickness (LVPWs), left ventricular posterior wall diastolic thickness (LVPWd) along with increased left ventricular systolic internal diameter (LVIDs) and left ventricular diastolic internal diameter (LVIDd) in DCM mice (Figure 7A–F). The expression levels of *OTUD1* in the DCM mouse hearts were evaluated via qPCR and Western blot. After Dox exposure, the *OTUD1* expression level in hearts of DCM group was significantly higher than
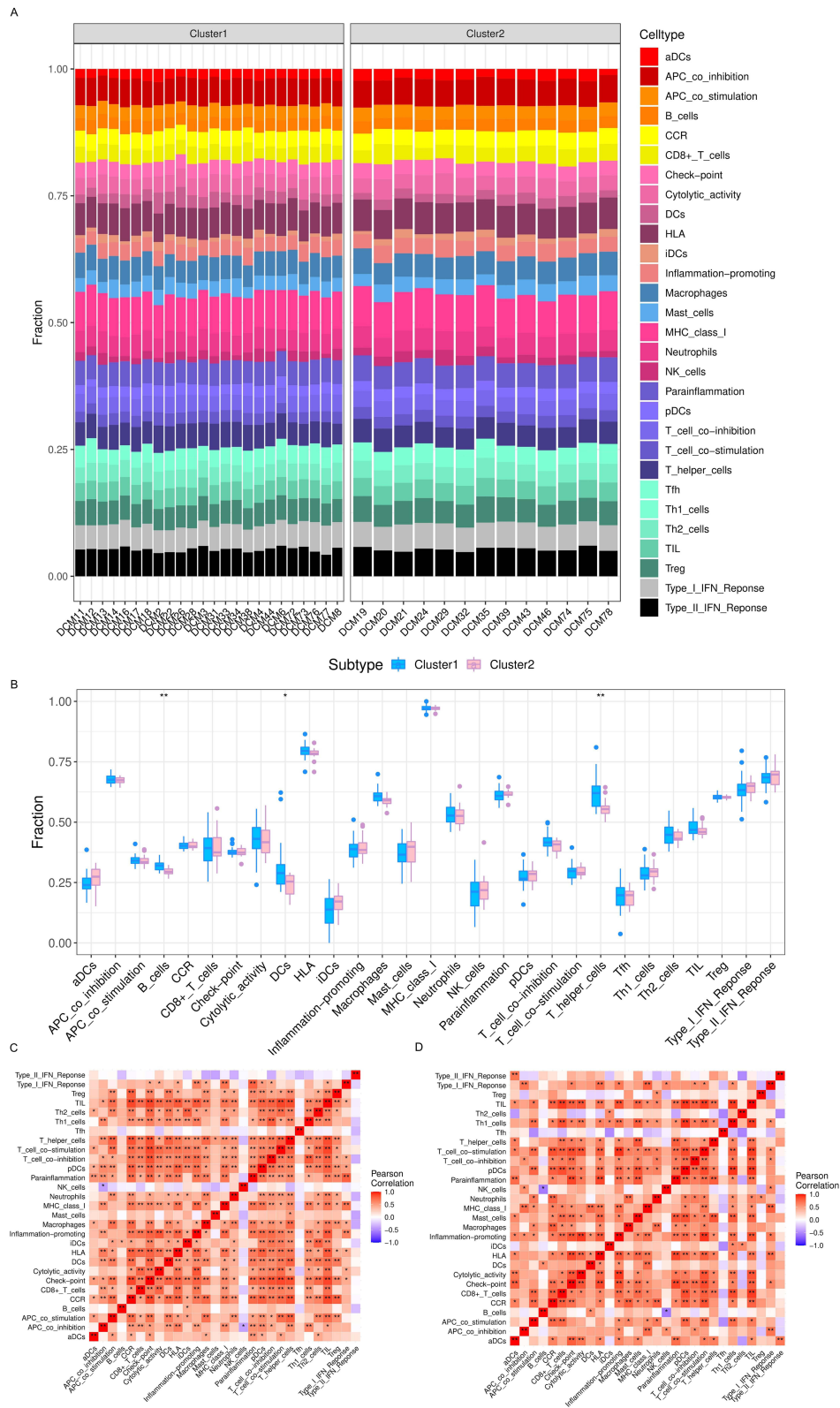
Figure 3 ssGSEA analysis of infiltrating immune cells between two clusters. (**A**) The difference of immune cells composition in each cluster; (**B**) the comparison of immune cells between the two clusters; (**C** and **D**) correlation matrix of immune cell proportions in cluster1(c) and cluster2(d). *p < 0.05, **p < 0.01.
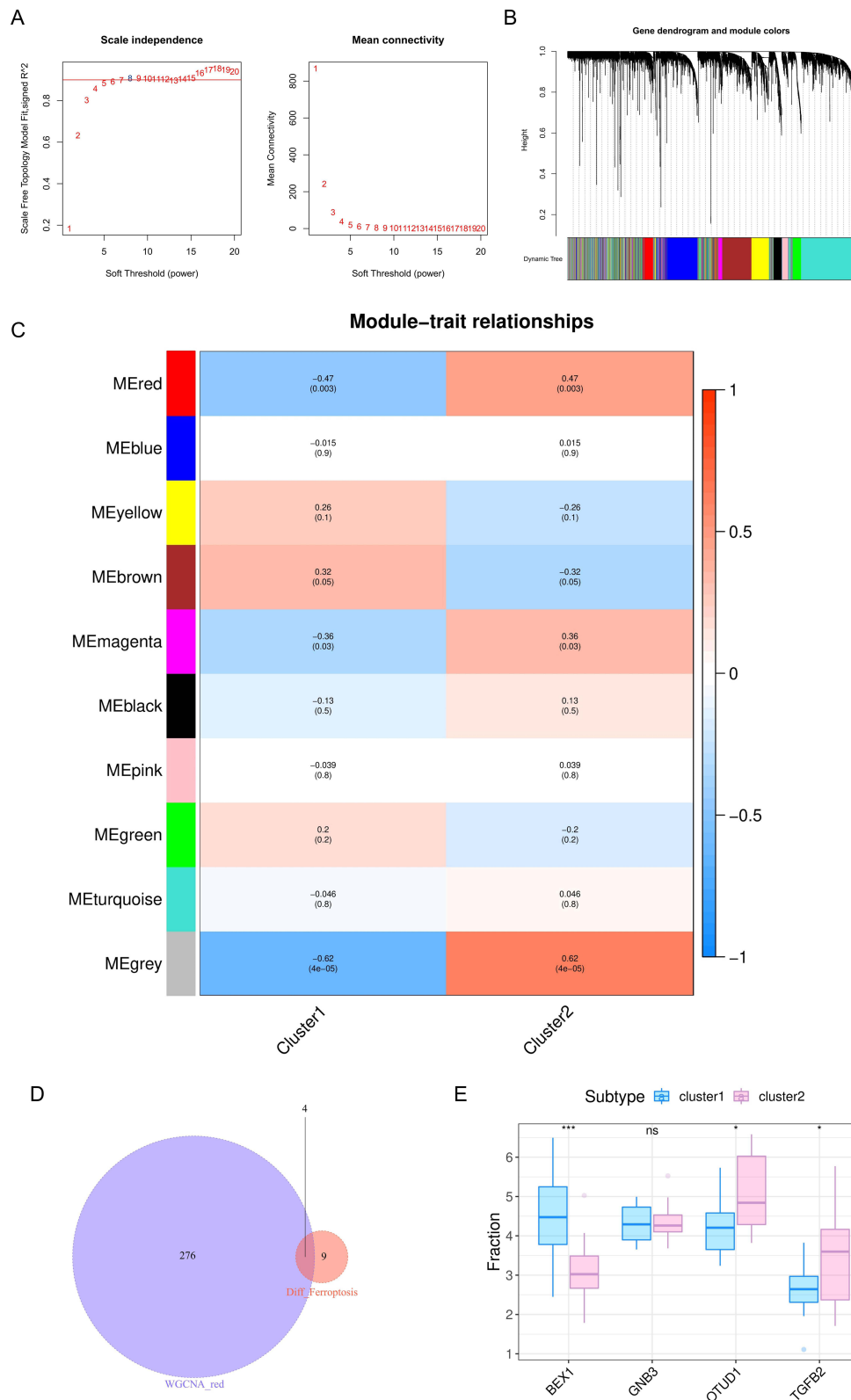
Figure 4 WGCNA module construction and key gene identification. (**A**) Analysis of network topology for soft-thresholding power; (**B**) gene clustering dendrogram: each branch represents a gene, and each color represents a co-expression module; (**C**) module-trait relationships heatmap, the red module was significantly associated with control;(**D**)a Venn diagram of genes in red module and ferroptosis-related DEGs (**E**) the expression of 4 hub genes between two clusters. *$p < 0.05$, ***$p < 0.001$.
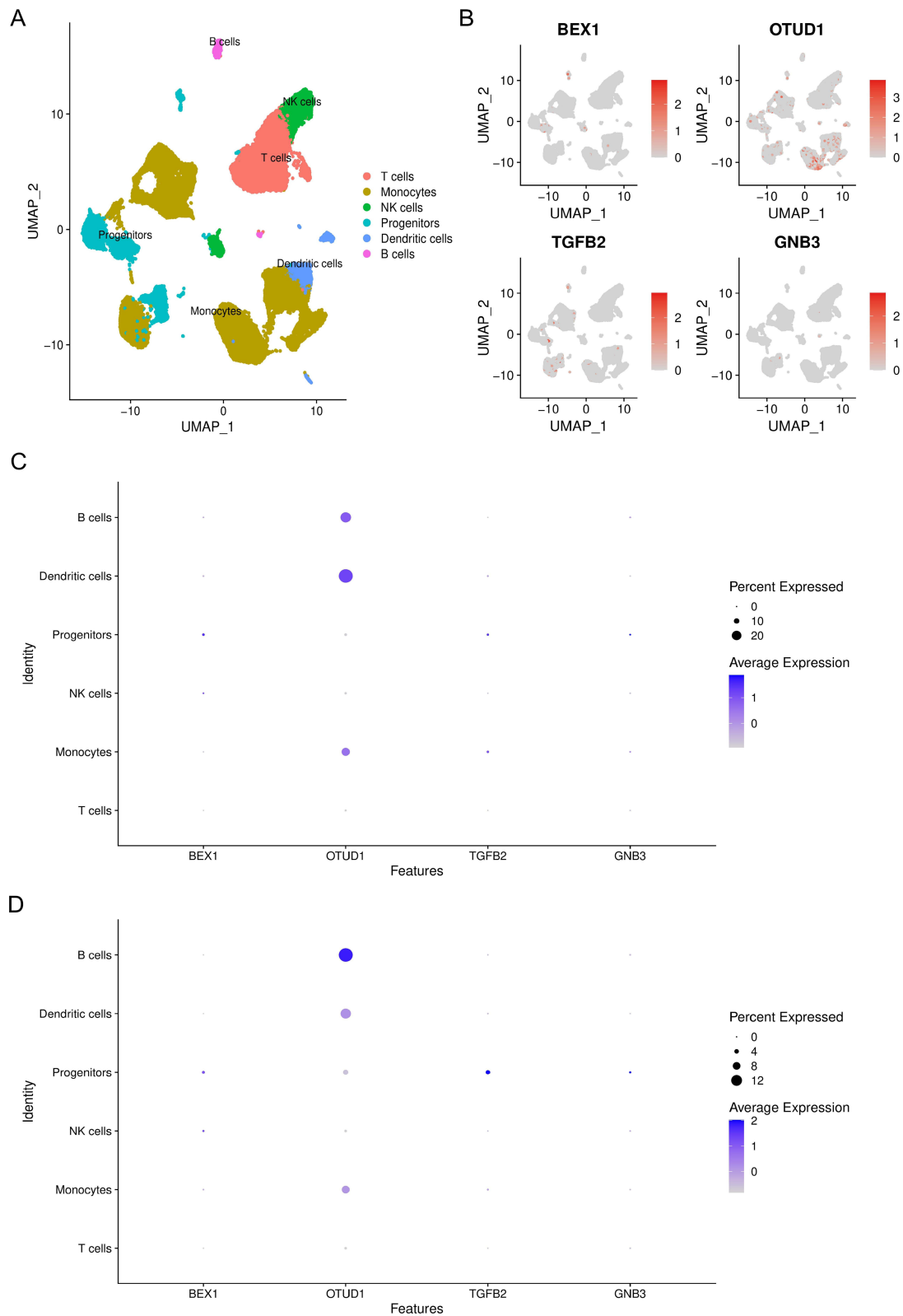
Figure 5 The orientation of hub genes in DCM patients' heart. (**A**) tSNE plots of immune cells pooled from sham and DCM patients; (**B**) the orientation of hub genes in patients' heart; (**C** and **D**) the expression percentage and level of hub genes in cardiac immune cells of sham (**C**) and DCM patients (**D**).
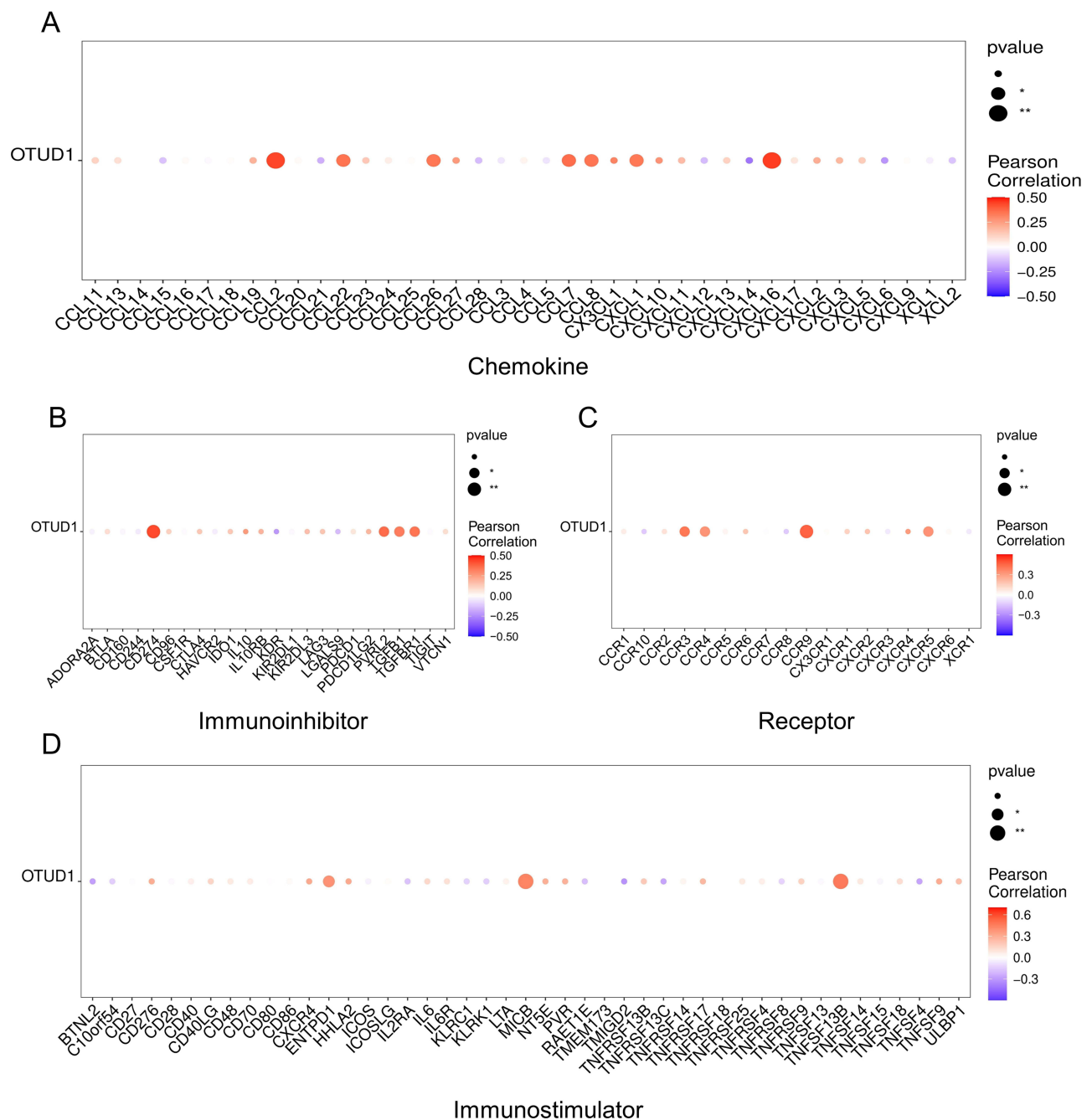
Figure 6 Immune characteristic of *OTUD1*. The relationship between *OTUD1* and chemokines (**A**), immunoinhibitor (**B**), immune receptor (**C**), and immune stimulators (**D**). *p < 0.05, **p < 0.01.

that in the controls (Figure 7G, I and K). Compared with the control group, the GSH/GSSG ratios and expression level of GPX4 in the DCM group were significantly decreased, while the number of 4-HNE positive cells increased, indicating the occurrence of ferroptosis in the heart of DCM mice (Figure 7G, H, J and L). As shown by immunostaining (Figure 7M), the colocation between *OTUD1* and CD11c and CD19 was identified in DCM mouse hearts, indicating *OTUD1* may play a role through B cells and DCs in DCM.
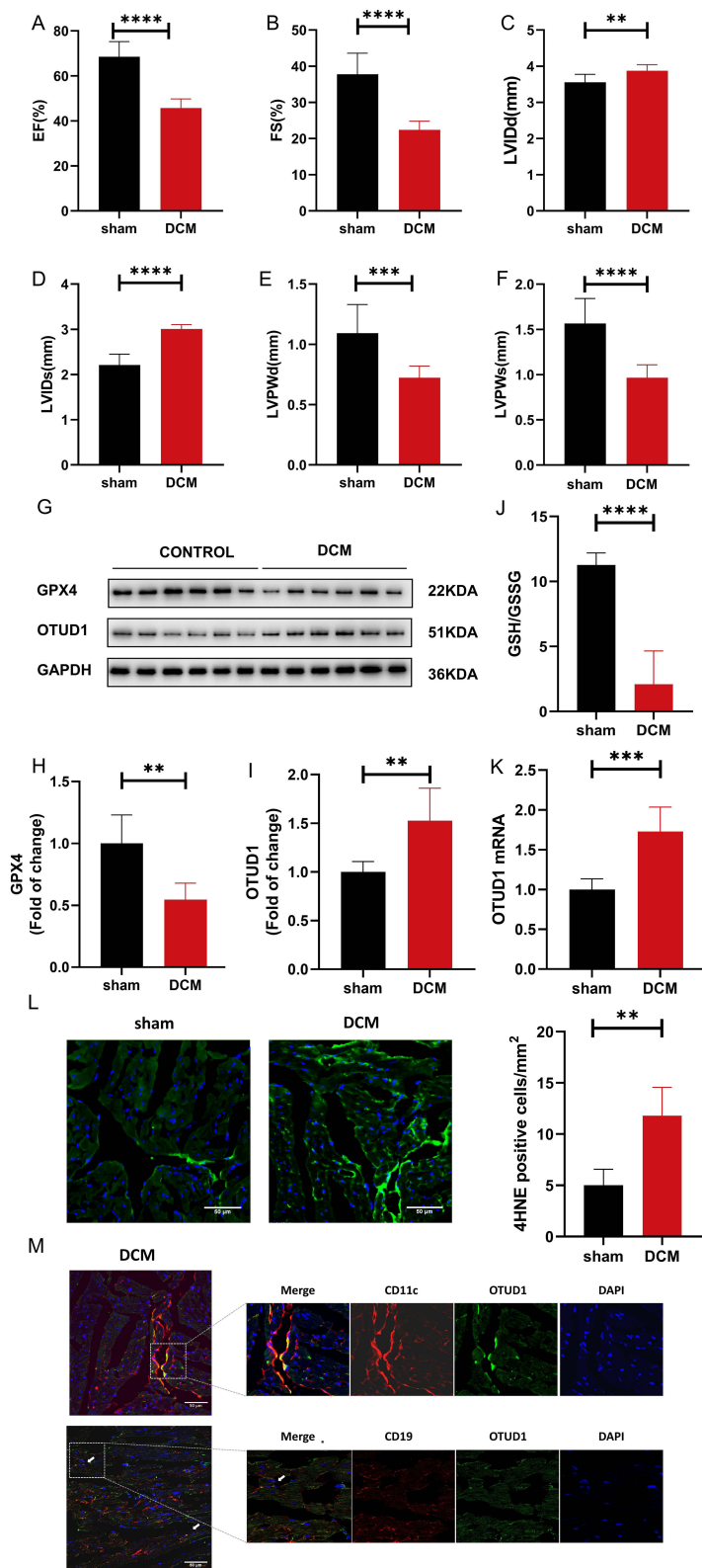
Figure 7 The verification of *OTUD1* in the heart of DCM mice. (**A-F**) Cardiac systolic function index (n=10 in each group); (**G-I**) representative WB bands and quantification of relative protein expression for GPX4 and *OTUD1* (n=6 in each group); (**J**) the GSH/GSSG ratio of sham and DCM mouse heart (n=6 in each group); (**K**) the expression level of *OTUD1* mRNA in the heart of DCM mouse (n=6 in each group). (**L**) Representative image of 4-hydroxynonenal staining in sham and DCM mouse hearts; (**M**) colocalization between *OTUD1* and CD11c and CD19 were analyzed by immunostaining in DCM mouse hearts. Data are shown as mean ± SD and were analyzed by a two-tailed unpaired *t*-test Ejection fraction (EF); shortening fraction (FS), left ventricular posterior wall systolic thickness (LVPWs); left ventricular posterior wall diastolic thickness (LVPWd); left ventricular systolic internal diameter (LVIDs); left ventricular diastolic internal diameter (LVIDd). **p < 0.01, ***p < 0.001 and ****p < 0.0001.

Discussion

As one of the most prevalent cardiomyopathies worldwide with structural and functional abnormalities, DCM often leads to higher mortality[18–20] and there is no effective treatment to prevent the progression of DCM. Ferroptosis is a novel type of regulated cell death triggered by iron-dependent lipid peroxidation, which is involved in a variety of cardiovascular diseases. For example, ferroptosis was evidenced in the heart of diabetic mice and it can be prevented by sulforaphane via AMPK/ NRF2 pathway.[21] Miyamoto et al also demonstrated iron overload via heme degradation in the endoplasmic reticulum will trigger ferroptosis in myocardial ischemia-reperfusion injury.[12] The heart is highly sensitive to energy metabolism and iron overload.[22] Ferroptosis can lead to the swelling and outer membrane rupture of mitochondria as well as accumulation of iron in the cells.[23,24] Therefore, ferroptosis may be a new direction for cardiovascular disease. However, the role of ferroptosis in DCM is still uncertain and further study is required. In our study, we screened 13 ferroptosis-related DEGs in DCM patients, and the functional analysis showed that these DEGs were engaged in the known mechanism of DCM such as cardiac muscle contraction, metabolism and extracellular matrix structural constituents.

It has been found that DCM patients can be divided into various subtypes, and there is significant heterogeneity in the different subtypes, including immune heterogeneity.[14] However, there is no effective treatment for heterogeneous DCM patients, and the majority of DCM patients have poor outcomes and prognosis.[18–20] Moreover, the mechanism of heterogeneity in DCM patients remains uncertain. Therefore, there is an urgent need to explore the mechanism of heterogeneity in DCM patients and to identify potential targets. In a variety of oncologic diseases, different expression patterns of ferroptosis have been found to strongly affect patients' prognosis. For example, molecular subtypes classified by ferroptosis-related genes are strongly associated with heterogeneity in patients with lung adenocarcinoma, and there are significant differences in prognosis and PD-L1 efficacy of patients with different subtypes.[17] Therefore, we constructed subtypes based on the expression of ferroptosis-related DEGs to explore the possible role of ferroptosis in DCM heterogeneity and finally divided the patients into two clusters.

DCM is a disease highly associated with the immune system, but the composition of the immune microenvironment in DCM has been controversial. Liang et al found that DCs increased in the hearts of patients with DCM and expressed more inflammation-related genes.[25] However, cardiac biopsies of patients with DCM showed a decrease in the number of DCs, especially in virus-positive heart samples.[26] The same paradox also occurs in B cells. The number of B cells was increased in the hearts of patients with DCM caused by viral myocarditis,[27] while another study showed a significant decrease in B cell markers in both congenital and autoimmune DCM.[28] It has been demonstrated that ferroptosis-related genes can lead to different immune infiltrates in many diseases. For example, patients in different clusters classified by the ferroptosis-related genes have different immune characteristic in osteosarcoma.[29] In our study, we also found immune infiltration differences in DCM patients between the different clusters. The immune pathway was highly enriched in cluster1 and the number of B cells, DC cells, and TH cells was also elevated in the hearts of these patients. Recent results have revealed that ferroptosis mediates the tumor suppressive activity of interferon gamma secreted by CD8+ T cells in response to immune checkpoint blockade.[30] At the same time, the truncated mutation of BNC1 will trigger ferroptosis through the NF2-YAP pathway and induce primary ovarian insufficiency.[31] In view of the fact that DCM is a widely acknowledged disease associated with a variety of genetic mutations and autoimmune, it is reasonable that ferroptosis might be regulated by various factors such as autoimmune, environment, genetics and therefore take part in the immune heterogeneity of DCM.

As a newly defined ferroptosis-related gene, *OTUD1* is receiving increasing attention for its role in immunity. In the intestinal lamina propria, the deletion of *OTUD1* will result in significantly increased numbers of DCs during dextran sulfate sodium treatment.[32] Previous research has revealed that *OTUD1* can promote iron transport ferroptosis via stabilizing IREB2 and thereby induce ferroptosis. At the same time, *OTUD1* also increases the release of damage-related molecular patterns (DAMPs) to recruit white blood cells and enhance the host immune response.[33] These results suggest that *OTUD1* may be a hub gene in the interaction between ferroptosis and immune infiltration. However, the role of *OTUD1* in heart remains unknown. We found that *OTUD1* was elevated in the heart of DCM mouse heart and may be a hub gene in the regulation of DCM immune infiltration by ferroptosis through DC cells and B cells, which had previously been shown to increase in cluster1. Moreover, the expression level of *OTUD1* was significantly different between the two clusters, indicating it may participate in

the heterogeneity of DCM. The increased expression level of *OTUD1* and colocation between *OTUD1* and B cells as well as DCs in the heart were verified in the DCM mouse model via Dox injection. In order to further elucidate the role of *OTUD1*, we analyzed the correlation between *OTUD1* and immune molecules and the most relevant factors were TNFSF13B, CCR9, CXCL16, CCL2, and CD274. TNFSF13B has been identified as B cell activator and was a potential biomarker for acute myocardial infarction.[34,35] In a mouse or cardiomyocyte hypertrophy model, the knockout of CCR9 will greatly attenuate cardiac hypertrophy.[36] CXCL16 can promote proliferation and impaired collagen synthesis in myocardial fibroblasts and ultimately results in the development of HF.[37] Guo et al have suggested the modulation of CCL2 signaling system might be a novel therapeutic strategy for DCM, while the blockade of CD274 will enhance cardiomyocyte inflammation and apoptosis via the activation of T cells.[38,39] In summary, these inflammatory factors were highly correlated with cardiac disease, but the relationship between these factors and DCM is almost unknown. The effect of *OTUD1* in DCM may be connected with these immune factors, and we provide some potential directions for the further investigation of *OTUD1* in the DCM.

Our study has several limitations. First, the small number of patients analyzed in this study may introduce bias. A larger sample size and a comprehensive analysis of different etiologies may better reveal the role of *OTUD1* as well as ferroptosis in the pathogenesis of DCM. Second, at present, there is no widely recognized animal model of DCM. We constructed a DCM mouse model by injecting Dox, which is a commonly used model. According to the results of cardiac echocardiography, the hearts of Dox-injected mice showed functional changes consistent with those of clinical DCM patients. Thus, our data are promising, but more animal models or even heart samples from DCM patients are still needed to validate the role of *OTUD1* in the DCM heart. Whether there are differences in immune infiltration and response to ferroptosis inhibitors in mouse models of DCM constructed for different etiologies still deserves further exploration. Furthermore, although we confirmed from animal models of DCM that *OTUD1* may be a potential target of DCM, it is necessary to knock out *OTUD1* in mice and observe the influence on cardiac ferroptosis and immune infiltration and *OTUD1* expression be validated in human heart samples. Third, the further mechanisms through which *OTUD1* contributes to DCM remain unknown, our data provided some direction for subsequent studies of *OTUD1* in the heart. As a key gene of ferroptosis and immune regulation, *OTUD1* is probably modulated by immune-related molecules such as TNFSF13B and CCR9, which in turn influence certain ferroptosis pathways and ultimately lead to the occurrence of ferroptosis. We suggest that future studies are necessary to examine whether there are differences in the cardiac immune microenvironment and ferroptosis markers in DCM patients with different etiologies. Besides, although Th cells were also shown to be significantly differentially expressed in the two clusters of DCM patients, our results did not find a relevant key gene. The role of Th cells in the immune heterogeneity of DCM patients needs to be further explored.

Conclusion

In summary, we found DCM patients classified by different expression patterns of ferroptosis-related DEGs had immune heterogeneity. We further identified *OTUD1* as a hub gene that may play a role in cardiac immune infiltration, particularly on DC cells and B cells, in DCM patients, providing a new target for subsequent studies of DCM.

Ethical Approval

The animal experiments were approved by the Animal Care and Use Committee of Guangdong Provincial People's Hospital (No. KY-Q-2022-366-01). The experiment complied with the Guide for the Care and Use of Laboratory Animals published by the US National Institutes of Health (NIH Publication No. 85-23, revised 1996).

Acknowledgments

Funding

Disclosure

The authors report no conflicts of interest in this work.

References

1. Weintraub RG, Semsarian C, Macdonald P. Dilated cardiomyopathy. *Lancet*. 2017;390(10092):400–414.
2. Feldtmann R, Kümmel A, Chamling B, et al. Myeloid differentiation factor-2 activates monocytes in patients with dilated cardiomyopathy. *Immunology*. 2022;167(1):40–53.
3. Sun X, Duan J, Gong C, et al. Colchicine ameliorates dilated cardiomyopathy via SIRT2-mediated suppression of NLRP3 inflammasome activation. *J Am Heart Assoc*. 2022;11(13):e025266.
4. Dávila-Román VG, Vedala G, Herrero P, et al. Altered myocardial fatty acid and glucose metabolism in idiopathic dilated cardiomyopathy. *J Am Coll Cardiol*. 2002;40(2):271–277.
5. Chen SN, Lombardi R, Karmouch J, et al. DNA damage response/TP53 pathway is activated and contributes to the pathogenesis of dilated cardiomyopathy associated with LMNA (Lamin A/C) mutations. *Circ Res*. 2019;124(6):856–873.
6. Caragnano A, Aleksova A, Bulfoni M, et al. Autophagy and inflammasome activation in dilated cardiomyopathy. *J Clin Med*. 2019;8(10):45.
7. Zeng C, Duan F, Hu J, et al. NLRP3 inflammasome-mediated pyroptosis contributes to the pathogenesis of non-ischemic dilated cardiomyopathy. *Redox Biol*. 2020;34:101523.
8. Li Y, Feng D, Wang Z, et al. Ischemia-induced ACSL4 activation contributes to ferroptosis-mediated tissue injury in intestinal ischemia/reperfusion. *Cell Death Differ*. 2019;26(11):2284–2299.
9. Tang D, Chen X, Kang R, Kroemer G. Ferroptosis: molecular mechanisms and health implications. *Cell Res*. 2021;31(2):107–125.
10. Wang J, Deng B, Liu Q, et al. Pyroptosis and ferroptosis induced by mixed lineage kinase 3 (MLK3) signaling in cardiomyocytes are essential for myocardial fibrosis in response to pressure overload. *Cell Death Dis*. 2020;11(7):574.
11. Zhang Y, Ren X, Wang Y, et al. Targeting ferroptosis by polydopamine nanoparticles protects heart against ischemia/reperfusion injury. *ACS Appl Mater Interfaces*. 2021;13(45):53671–53682.
12. Miyamoto HD, Ikeda M, Ide T, et al. Iron overload via heme degradation in the endoplasmic reticulum triggers ferroptosis in myocardial ischemia-reperfusion injury. *JACC Basic Transl Sci*. 2022;7(8):800–819.
13. Wang Z, Xia Q, Su W, et al. Exploring the communal pathogenesis, ferroptosis mechanism, and potential therapeutic targets of dilated cardiomyopathy and hypertrophic cardiomyopathy via a microarray data analysis. *Front Cardiovasc Med*. 2022;9:824756.
14. Verdonschot JAJ, Merlo M, Dominguez F, et al. Phenotypic clustering of dilated cardiomyopathy patients highlights important pathophysiological differences. *Eur Heart J*. 2021;42(2):162–174.
15. Mattson DL. Immune mechanisms of salt-sensitive hypertension and renal end-organ damage. *Nat Rev Nephrol*. 2019;15(5):290–300.
16. Jia Q, Chu H, Jin Z, Long H, Zhu B. High-throughput single-cell sequencing in cancer research. *Signal Transduct Target Ther*. 2022;7(1):145.
17. Zhang W, Yao S, Huang H, et al. Molecular subtypes based on ferroptosis-related genes and tumor microenvironment infiltration characterization in lung adenocarcinoma. *Oncoimmunology*. 2021;10(1):1959977.
18. Li S, Wang Y, Yang W, et al. Cardiac MRI risk stratification for dilated cardiomyopathy with left ventricular ejection fraction of 35% or higher. *Radiology*. 2022;213059.
19. Tang HS, Kwan CT, He J, et al. Prognostic utility of cardiac MRI myocardial strain parameters in patients with ischemic and nonischemic dilated cardiomyopathy: a multicenter study. *AJR Am J Roentgenol*. 2022:56.
20. Wu HS, Dong JZ, Du X, et al. Risk factors for left ventricular thrombus formation in patients with dilated cardiomyopathy. *Semin Thromb Hemost*. 2022:345.
21. Wang X, Chen X, Zhou W, et al. Ferroptosis is essential for diabetic cardiomyopathy and is prevented by sulforaphane via AMPK/NRF2 pathways. *Acta Pharm Sin B*. 2022;12(2):708–722.
22. Fang X, Ardehali H, Min J, Wang F. The molecular and metabolic landscape of iron and ferroptosis in cardiovascular disease. *Nat Rev Cardiol*. 2023;20(1):7–23.
23. Fang X, Wang H, Han D, et al. Ferroptosis as a target for protection against cardiomyopathy. *Proc Natl Acad Sci U S A*. 2019;116(7):2672–2680.
24. Kwon MY, Park E, Lee SJ, Chung SW. Heme oxygenase-1 accelerates erastin-induced ferroptotic cell death. *Oncotarget*. 2015;6(27):24393–24403.
25. Liang L, Sun J, Teng T, et al. Expression profile of inflammation response genes and potential regulatory mechanisms in dilated cardiomyopathy. *Oxid Med Cell Longev*. 2022;2022:1051652.
26. Pistulli R, König S, Drobnik S, et al. Decrease in dendritic cells in endomyocardial biopsies of human dilated cardiomyopathy. *Eur J Heart Fail*. 2013;15(9):974–985.
27. Yuan J, Cao AL, Yu M, et al. Th17 cells facilitate the humoral immune response in patients with acute viral myocarditis. *J Clin Immunol*. 2010;30(2):226–234.
28. Nield LE, von Both I, Popel N, et al. Comparison of immune profiles in fetal hearts with idiopathic dilated cardiomyopathy, maternal autoimmune-associated dilated cardiomyopathy and the normal fetus. *Pediatr Cardiol*. 2016;37(2):353–363.
29. Lei T, Qian H, Lei P, Hu Y. Ferroptosis-related gene signature associates with immunity and predicts prognosis accurately in patients with osteosarcoma. *Cancer Sci*. 2021;112(11):4785–4798.
30. Stockwell BR, Jiang X. A physiological function for ferroptosis in tumor suppression by the immune system. *Cell Metab*. 2019;30(1):14–15.
31. Wang F, Liu Y, Ni F, et al. BNC1 deficiency-triggered ferroptosis through the NF2-YAP pathway induces primary ovarian insufficiency. *Nat Commun*. 2022;13(1):5871.
32. Wu B, Qiang L, Zhang Y, et al. The deubiquitinase OTUD1 inhibits colonic inflammation by suppressing RIPK1-mediated NF-κB signaling. *Cell Mol Immunol*. 2022;19(2):276–289.
33. Song J, Liu T, Yin Y, et al. The deubiquitinase OTUD1 enhances iron transport and potentiates host antitumor immunity. *EMBO Rep*. 2021;22(2):e51162.
34. McClure M, Gopaluni S, Jayne D, Jones R. B cell therapy in ANCA-associated vasculitis: current and emerging treatment options. *Nat Rev Rheumatol*. 2018;14(10):580–591.

35. Zouggari Y, Ait-Oufella H, Bonnin P, et al. B lymphocytes trigger monocyte mobilization and impair heart function after acute myocardial infarction. *Nat Med*. 2013;19(10):1273–1280.

36. Xu Z, Mei F, Liu H, Sun C, Zheng Z. C-C Motif Chemokine Receptor 9 exacerbates pressure overload-induced cardiac hypertrophy and dysfunction. *J Am Heart Assoc*. 2016;5(5):453.

37. Dahl CP, Husberg C, Gullestad L, et al. Increased production of CXCL16 in experimental and clinical heart failure: a possible role in extracellular matrix remodeling. *Circ Heart Fail*. 2009;2(6):624–632.

38. Guo J, Zhang H, Xiao J, et al. Monocyte chemotactic protein-1 promotes the myocardial homing of mesenchymal stem cells in dilated cardiomyopathy. *Int J Mol Sci*. 2013;14(4):8164–8178.

39. Tay WT, Fang YH, Beh ST, et al. Programmed Cell Death-1: programmed Cell Death-Ligand 1 interaction protects human cardiomyocytes against T-cell mediated inflammation and apoptosis response in vitro. *Int J Mol Sci*. 2020;21(7):23.